External Award 06HQGR0010
Panel EP

# EVALUATION OF ANALYTICAL PROCEDURES FOR ESTIMATING SEISMICALLY INDUCED PERMANENT DEFORMATION IN SLOPES


Principal Investigator:
**Joseph Wartman**

Graduate Student Researcher:
**Patrick M. Strenk**

Drexel University
3141 Chestnut Street, Philadelphia, PA 19104 USA

joseph.wartman@drexel.edu



*Research supported by the U.S. Geological Survey (USGS), Department of the Interior, under USGS award number 20040212. The views and conclusions contained in this document are those of the authors and should not be interpreted as necessarily representing the official policies, either expressed or implied, of the U.S. Government.*

**CONTENTS**

TECHNICAL ABSTRACT……..……ii

NON-TECHNICAL SUMMARY……..……iii

INTRODUCTION…….……...1

VALIDITY OF THE PSEUDOSTATIC SURFACE…….....1

Background……...1

Earthquake Ground Motions…….2

Fully-Coupled Dynamic Analyses……....2

Slope Geometry and Material Properties……..……..…2

Pseudostatic Analyses……...……3

1D Soil Column Analysis……..……..……5

Description of Critical Surface Geometry……....……..6

Results……...……6

1D Analysis Results……..……6

2D Analysis Results……..……7

Discussion and Conclusions…….……7

ACCURACY OF DEFORMATION-BASED PROCEDURES……..9

Dynamic Response Validation of *FLAC*……..9

Characterization of Seismic Resistance and Demand using Monte-Carlo……...……..10

Seismic Resistance…….11

Seismic Demand……12

Deformation-Based Procedures……..13

Method Implementation…….14

Case History Analysis…….15

Subsurface Conditions & Soil Properties…….20

Deformation……..……20

Ground Motions Characterization……21

Uncertain Parameters……...22

Deformation-Based Analyses……..24

Discussion and Conclusions……24

Project Publications…….25

REFERENCES……...……..25

APPENDIX A - Deformation-Based Procedure References

External Award 06HQGR0010
Panel EP

# EVALUATION OF ANALYTICAL PROCEDURES FOR ESTIMATING SEISMICALLY INDUCED PERMANENT DEFORMATION IN SLOPES

Joseph Wartman

Drexel University
3141 Chestnut Street, Philadelphia, PA 19104 USA
joseph.wartman@drexel.edu

## TECHNICAL ABSTRACT

Recently, attention has been focused on the development and refinement of analytical procedures for estimating seismically induced permanent deformations in landslides and earth structures. The continued evolution of these procedures has led to a significant amount of confusion in the seismic hazard community that has centered mainly on issues of method applicability, accuracy and validity. Moreover, implementation of some of these methods still requires that a limit-equilibrium pseudostatic analysis be performed to quantify the seismic resistance and to determine the geometry of the critical slip surface. Such an a priori assumption of the critical surface is questionable since it is recognized that both dynamic response and sliding response are a coupled phenomena in real slopes. In the first phase of this research, the validity of this pseudostatic assumption was investigated by performing a series of 1D and 2D dynamic analyses to evaluate how changes in dynamic response influence the geometry of the failure mechanism. In the second phase, a probabilistic Monte-Carlo approach was developed to systematically assess the accuracy and applicability of a suite deformation-based procedures used to predict seismically induced deformations in slopes. This approach was used to assess the predictive capabilities of each deformation-based method by comparing them to a series of well-documented case histories of actual earthquake-induced displacement.

External Award 06HQGR0010
Panel EP

# EVALUATION OF ANALYTICAL PROCEDURES FOR ESTIMATING SEISMICALLY INDUCED PERMANENT DEFORMATION IN SLOPES

Joseph Wartman

Drexel University
3141 Chestnut Street, Philadelphia, PA 19104 USA
joseph.wartman@drexel.edu

## NON-TECHNICAL SUMMARY

Continued development and refinement of analytical procedures for estimating seismically induced permanent deformations in landslides and earth structures has resulted in a considerable amount of confusion in the seismic hazard community. Of particular concern are issues of method applicability, accuracy and validity. Moreover, several of these deformation-based procedures make an a priori assumption about the geometry of the critical failure surface on which deformations are assumed to occur. A probabilistic approach is used to assess the predictive capabilities of 16 available deformation-based procedures by comparing them to a series of well-documented case histories of actual earthquake-induced. The validity of the a priori surface assumption was investigated by performing a series of dynamic simulations on a simple, homogeneous slope model.

## INTRODUCTION

In recent years attention has been focused on the development and refinement of analytical procedures for estimating seismically induced permanent deformations in slopes. Today, practitioners and researchers have an array of increasingly sophisticated deformation-based procedures from which to choose when assessing the seismic stability of slopes. Some of these deformation-based analytical procedures have been compared and/or calibrated against small-scale laboratory tests (e.g. centrifuge, shaking table); however, there have been few attempts to assess the accuracy and applicability of these procedures against well documented case histories of earthquake-induced deformations in actual slopes.

In the current project we examined the applicability of several analytical procedures for estimating seismically induced deformations by applying and comparing these methodologies against well-documented case histories. Early in the work we identified a fundamental concern with the way that the "critical" slide surface is identified and used in the various analyses. Specifically, we noted that this surface is typically identified using a pseudostatic analysis, which neglects the dynamic response that develops in a slope, and which can give rise to the development of other slip surfaces. Accordingly, in the first phase of this work we undertook and investigation of this issue. In the second phase we compare a suite of seismic displacement methodologies to the actual performance of several well documented slopes.

## VALIDITY OF THE PSEUDOSTATIC SURFACE

### Background

Since the post-earthquake serviceability of slopes is controlled by deformations, analysis procedures that predict the magnitude of these deformations provide a useful indication of seismic slope stability. Newmark (1965) developed the first of these deformation-based methods. Implementation of this method requires two parameters: the value of the seismic yield coefficient ($k_y$) [determined from a limit-equilibrium (LEM) based pseudostatic analysis] and an acceleration time history at the base of the earth structure. Permanent deformations are evaluated through double integration of accelerations in excess of the $k_y$ value and are assumed to accumulate on the critical failure surface obtained from the pseudostatic analysis.

By using a base input acceleration time history in Newmark's method it is assumed that the slide mass (as well as the entire earth structure) is non-compliant and thus unresponsive to dynamic loading. This simplifying assumption represents the method's main limitation in that rigid body behavior implies that the accelerations within the earth structure and slide mass are the same as those in the foundation material below the structure.

Clearly, this assumption is not a realistic one; the materials that comprise earth structures are in fact compliant and respond dynamically as deformable bodies to ground motions. As the motion propagates, different parts of an earth structure move by different amounts and with different phases, thereby creating a distribution of accelerations throughout the structure that vary in space and time. Correspondingly, it follows that the destabilizing inertial forces acting on a given slide mass will not be proportional to the acceleration at any one point within the slide mass (Chopra 1967). Recognition of this has lead to the development of an enhanced deformation-based method, the so-called decoupled method that incorporates the effect of dynamic response by expressing the seismic loading experienced by the slide mass as a horizontal equivalent acceleration (*HEA*) (Makdisi & Seed 1978). However, an important limitation of this method is that the dynamic response analysis is decoupled from the subsequent double-integration of the *HEA* time history in a separate two-step process.

Conceptually, the transition from rigid-block methods to decoupled procedures mark an improvement in evaluation of the seismic demand that a slide mass will experience. However, implementation of these

deformation-based procedures still requires that a limit-equilibrium analysis be performed to determine $k_y$ and the critical pseudostatic surface. Such an a priori assumption of the critical surface is questionable since it is recognized that both dynamic response and sliding response are a coupled phenomena in real slopes (Kramer & Smith 1997). Moreover, this assumption implies that dynamic response does not affect the nature of the failure mechanism. However, if the critical surface were allowed to develop freely in response to the dynamic response of the earth structure, then a different mechanism might develop.

This phase of the research work examines the commonly made assumption that the "critical" surface determined from a pseudostatic analysis is the same as that under dynamic conditions. To that end, slope models were subjected to a variety of dynamic loading conditions to evaluate and quantify how the dynamic response of the system affects the geometry of the resulting failure mechanism.

Earthquake Ground Motions

In order to examine the effect of dynamic response it was necessary to first develop a database of ground motions that exhibited a wide range of frequency contents. The ground motions used in this study consist of 124 free-field outcrop recordings from 24 earthquake events. The duration of the ground motions vary from 10 to 150 s. The frequency content of each motion was characterized by the mean-square frequency ($f_m$) and ranges between 0.85 and 8.08 Hz. This parameter was selected over other measures such as the predominant frequency ($f_p$) and Newmark-Hall frequency ($f_{V|A}$) since it has the advantage of being based on a larger portion of the frequency range of the record in its calculation (Rathje et al. 1998). In addition, 7 single frequency sine motions were also used in this study. These motions consist of a 10 s interval of constant amplitude with 5 s ramp at the beginning and end of the motion. The frequency of these motions ranged from 1.25 to 5.0 Hz.

Fully-Coupled Dynamic Analyses

For these analyses, a variety of dynamic conditions were evaluated by subjecting a 1D soil column and a 2D slope model to the database of ground motions for a range of shear wave velocity values. Details of these analyses are described below.

*Slope Geometry and Material Properties*

The model consists of a simple slope with a total height ($H$) of 40 m and a 20 m thick foundation layer; the slope face is inclined at an angle ($\beta$) of 30$^o$ (Fig. 1). The model was constructed using a square mesh with an average zone size of 0.75 m; a square mesh has been shown to have a minimal effect on the geometry of the failure mechanism for homogeneous simple slopes (Shukha & Baker 2003). A separate sensitivity analysis evaluating mesh type confirmed these results. The lateral boundaries of the grid were modeled as a free-field and were extended beyond the slope area to minimize the influence on dynamic response.

Two material types were evaluated: frictional-cohesive and purely cohesive. For the frictional-cohesive case, the material was modeled with the strain-softening constitutive model with peak strength parameters of $\phi = 30^o$ and $c$ = 10 kPa. A low level of sensitivity was used ($SI$ = 1.05) to enhance localization of the failure mechanism (Griffiths & Kidger 1995). For the cohesive case, the soil was modeled as a Mohr-Coulomb material with an undrained strength ($s_u$) that increased with depth ($s_u/p$ = 0.33, $\phi = 0^o$). Both materials were assigned a unit weight ($\gamma$) of 20 kN/m$^3$ and a Poisson's ratio ($\nu$) of 0.3. In the interest of better modeling plastic behavior by avoiding problems of excessive dilation, the frictional-cohesive soil was modeled with a non-associative flow rule (dilation angle, $\psi = 0^o$).

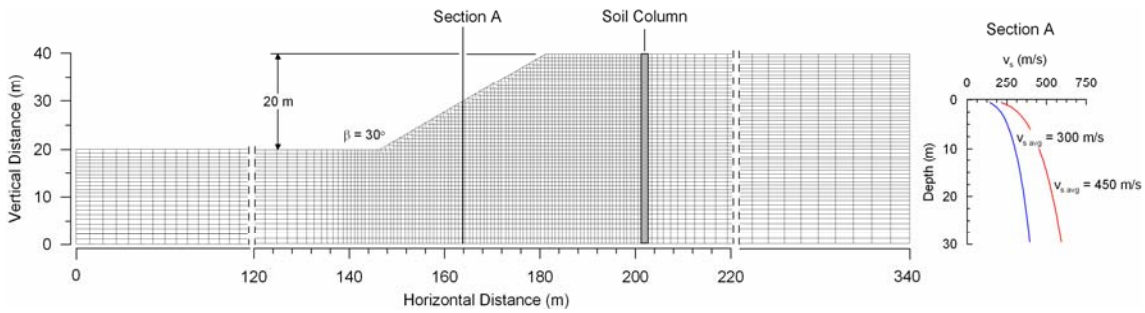


**Figure 1.** Slope and soil column models.

A varied shear wave velocity ($v_s$) profile (increases with depth) was implemented in the model and defined according to the Seed & Idriss (1970) relationship that relates initial shear modulus ($G_{max}$) to the mean effective stress ($\sigma_m'$):

$$G_{max} = 21.7\, p_a\, K \left( \frac{\sigma_m'}{p_a} \right)^n \qquad \text{(Eqn. 1)}$$

where $p_a$ = atmospheric pressure; $K$ = constant (related to void ratio and density); and $n$ = exponent. Elastic properties were updated within the model based on the in-situ stress state determined by the static solution. Two profiles were used with average shear wave velocities ($v_{s\,avg}$) of 300 m/s (K = 60, n = 0.5) and 450 m/s (K = 135, n = 0.5) (Fig. 1). The value of $v_{s\,avg}$ was calculated according to the following equation (ICC 2006):

$$v_{s\,avg} = \sum_{i=1}^{n} d_i \Big/ \sum_{i=1}^{n} \frac{d_i}{v_{si}} \qquad \text{(Eqn. 2)}$$

where $v_{si}$ = shear wave velocity at pre-determined layers and $d_i$ = thickness of each layer.

The ground motions were applied as shear stress time histories in order to model the bottom of the slope as a quiet absorbing boundary. Material damping was modeled with a Rayleigh damping scheme ($\xi$ = 2.5% at $f_m$ of the ground motion). A lower $\xi$ value was selected for these analyses to enhance the response of the slope and increase computational efficiency. Moreover, higher damping was deemed unnecessary considering the additional energy loss associated with shear yielding in the slope area. It should be noted that when the damping response curves are defined based on a single frequency point, lower $f_m$ values can lead to over-damped conditions in the model. However, the effect of this was assumed to be small given the reduced level of damping used. Also note that the amplitude of all ground motions were uniformly scaled to be roughly 10% higher than the LEM $k_y$ value for each soil model to ensure that failure was triggered.

*Pseudostatic Analyses*

As an initial step, the $k_y$ value and critical surface for the two soil models were determined using *FLAC* (Itasca 2005). These results were then compared with the LEM solution obtained using Spencer's method (Spencer 1967). In order for a compatible comparison with the LEM results, the Mohr-Coulomb model was used for the frictional-cohesive case.

Using *FLAC*, a technique we term "pseudostatic stepping" was implemented using a *FISH* function that incrementally increases the horizontal component of gravitational acceleration applied to the model. For each increment, grid point displacements along the crest of the slope are recorded as the model is brought to equilibrium. Instability was signaled by the occurrence of excessive displacement along the slope

crest; a threshold value of 1% of the slope height (above the foundation layer) was used as the criteria to detect failure.

The results for the frictional-cohesive case are shown in Figure 2. It is clear that on the verge of instability, the maximum crest displacement suddenly increases for a small change in the horizontal acceleration, a point that corresponds to the seismic yield coefficient.

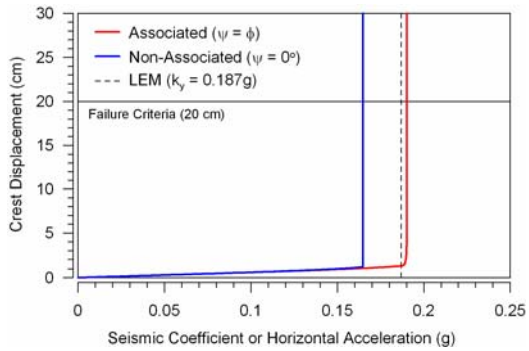


**Figure 2.** Results for *FLAC* pseudostatic analysis (for frictional-cohesive soil)

The $k_y$ values calculated by this method are shown in Table 1. Sensitivity analyses evaluating the effect of dilation angle ($\psi$) for the frictional-cohesive soil indicated that a closer match to the LEM $k_y$ value was attained for higher $\psi$ (up to the condition of normality, $\phi = \psi$). Depending on the flow rule assumption, the $k_y$ values for the frictional-cohesive soil were between 2% higher and 12% lower than those calculated by LEM. For the cohesive soil, the $k_y$ value obtained from *FLAC* was approximately 10% lower than LEM.

**Table 1.** Comparison of the seismic yield coefficient

| Soil Model | LEM | *FLAC* | |
|---|---|---|---|
| | | $k_y$ (for $\psi = \phi$) | $k_y$ (for $\psi = 0^o$) |
| Frictional-cohesive | 0.187 g | 0.190 g | 0.165 g |
| Purely cohesive | 0.101 g | 0.091 g | 0.091 g |

Figure 3 compares the critical surfaces obtained by this method with that obtained by LEM. Since *FLAC* is not restricted by the circular arc assumption as in LEM, surfaces are generally similar (but not identical) to the pseudostatic LEM surface. In addition, the effect of using a non-associated flow rule is clearly evident in the difference between the failure mechanisms for the frictional-cohesive case. Differences between the surfaces are also apparent for the cohesive case, specifically near the toe of the slope. This is likely due to the fundamentally different methods used by LEM and *FLAC* to calculate the model stresses and strength variation ($s_u/p$).

For the frictional-cohesive soil, the lower $k_y$ value calculated using *FLAC* are reasonable considering that the collapse load of a material with a non-associative flow rule is generally smaller than that of a material with an associative flow rule (Chen 1975). The assumption of an associated flow rule implies that dilation occurs during shear failure however, the magnitude of this volume change is far greater than is ever observed experimentally for frictional soils (Vermeer & de Borst, 1984). As such it is reasonable that different failure mechanisms would develop for such fundamentally different material behaviors. However, for the same failure mode, it has been shown that identical results for the collapse load can be obtained by upper bound limit analysis (where $\phi = \psi$ is assumed) and limit-equilibrium (e.g. Drescher & Detournay 1993). In such cases, the LEM solution can be regarded as a special form of the upper bound

solution. Thus for an associated flow rule, closer agreement between the failure mechanisms and collapse loads predicted by *FLAC* and LEM can be expected (Figs 2, 3).

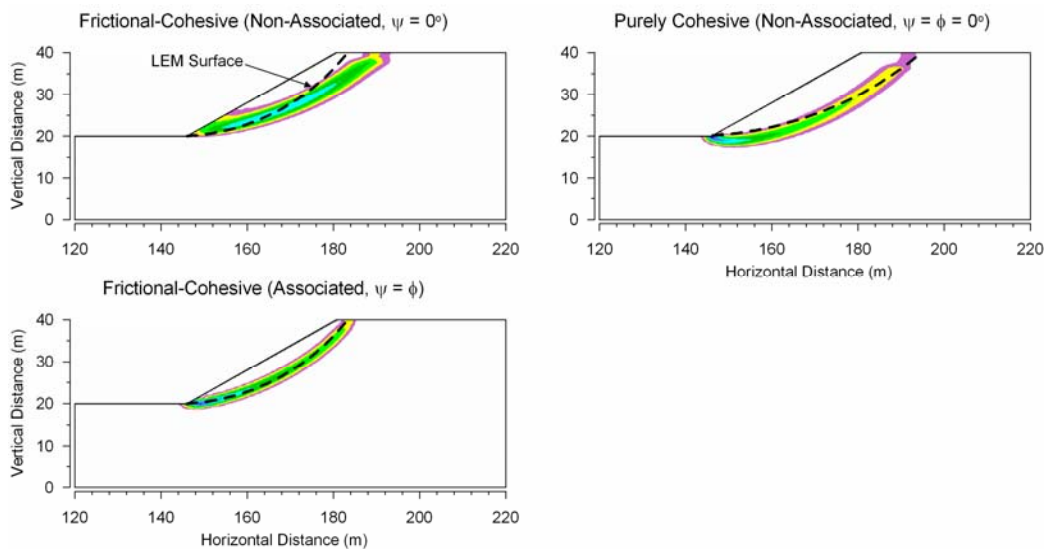


**Figure 3.** Comparison of the critical pseudostatic surfaces

*1D Soil Column Analysis*

A preliminary investigation of the influence of dynamic response on the failure mechanism was evaluated through a series of 1D dynamic analyses of a 40 m soil column consisting of 80 zones. The representative location of the soil column within the slope model is shown in Figure 1. The soil column was modeled as a linear, elastic material with elastic properties that varied with depth according to the selected shear wave velocity profile; four profiles were used in the 1D analyses ($v_{s\ avg}$ = 150 - 600 m/s). To be consistent with the slope model, a quiet absorbing boundary was implemented at the bottom of the soil column and material damping was modeled with the same Rayleigh damping scheme.

The seismic loading on a potential sliding mass can be represented by the horizontal equivalent acceleration (*HEA)* (Chopra 1967). The *HEA* essentially represents the integration of all the acceleration time histories within a slide mass and for 1D conditions can be expressed as:

$$HEA(t) = \frac{\tau(t)}{\sigma_v} g \qquad \text{(Eqn. 3)}$$

where $\tau(t)$ = horizontal shear stress time history acting at the depth of the sliding surface and $\sigma_v$ = total stress at the depth of the surface; and $g$ = acceleration due to gravity. By this definition, $HEA(t)$ can be thought of as the equivalent lateral acceleration required to produce the same shear stress $\tau(t)$ at that depth, and in this way represents a spatial average of the accelerations acting within the slide mass. A *FISH* function was used to calculate the *HEA* time history at each zone in the soil column. Since shear stresses are zone quantities in *FLAC*, it was assumed that the location of the slip surface corresponds to the bottom boundary of the zone in which shear stresses were evaluated. The seismic yield coefficient ($k_y$) for different slip surfaces was calculated based on a definition analogous to that for *HEA* given by Equation (3). For a potential surface at some depth, $k_y$ was calculated as:

$$k_y = \frac{\tau_{max}(z)}{\sigma_v} g \qquad \text{(Eqn. 4)}$$

where $\tau_{max}(z)$ = available soil strength along a potential slip surface at some depth ($z$). By this definition, $k_y$ represents the minimum acceleration required to exceed the strength of the material along the slip surface. The $\tau_{max}$ value used in this calculation was based on the frictional-cohesive soil model only. The results of these analyses are presented and discussed in subsequent sections.

*Description of Critical Surface Geometry*

The failure mechanisms obtained from the 2D dynamic and pseudostatic analyses is indicated by a localized zone of intense shear strain accumulation. As such, it was necessary to develop a method to extract and analyze the slip surface geometry in systematic manner. To that end, a routine was written in *MATLAB* (Mathworks 2007) that utilizes the shear strain increment (ssi) data exported from each analysis. In this routine, a non-linear Gauss-Newton least-squares approach was used to fit a circular arc to the x/y coordinate locations of the ssi data that were within some percentage of the peak strain value. The choice of a circular arc to fit the observed failure mechanism was justified because this surface type is a reasonable approximation for homogeneous slopes. However for the case of the purely cohesive soil, the failure mechanisms predicted by *FLAC* appeared to be more log-spiral which resulted in a slightly less accurate match in the vicinity of the toe of the surface. In addition to determining the location of the center point ($x_c$, $y_c$) and the radius ($R$) of the best-fit circular surface, the routine characterized the geometry even further according to several descriptors shown in Figure 4. These include: maximum slide mass thickness ($h$); slide mass volume ($V$) (per unit length of slope); crest distance ($D$); and intercept chord angle ($\eta$).

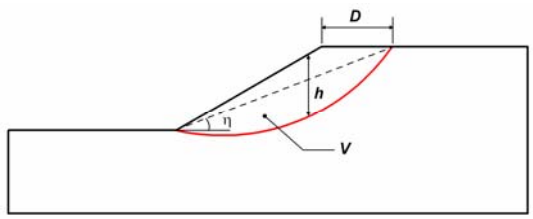


**Figure 4.** Surface descriptors

Results

In general, the dynamic response of a system is a function of the model geometry, material stiffness (defined by $v_{s\ avg}$) and the frequency content of the ground motion, in this case characterized by $f_m$. The various dynamic conditions evaluated with the 1D and 2D dynamic analyses were conveniently expressed as the wavelength ratio ($\lambda/H$) calculated as:

$$\frac{\lambda}{H} = \frac{v_{s\ avg}}{f_m H} \qquad \text{(Eqn. 5)}$$

where $H$ = total height of the soil column or slope model. Based on the number of ground motions in the database as well as the $v_s$ profiles considered, over 450 different dynamic conditions were evaluated in the 1D soil column analyses. For the 2D coupled analyses, approximately 250 conditions for each soil model were evaluated.

*1D Analysis Results*

For each soil column analysis, 80 *HEA* time histories were exported. Using a routine written with *MATLAB* the peak value ($k_{max}$) of each of the *HEA* time history was calculated along with the corresponding seismic yield coefficient ($k_y$). For each potential slip surface along the height of the column, the resistance was normalized with respect to the seismic demand to determine the stability ratio

($k_y/k_{max}$). The depth where the stability ratio is a minimum indicates the slip surface that is most unstable (i.e. critical surface).

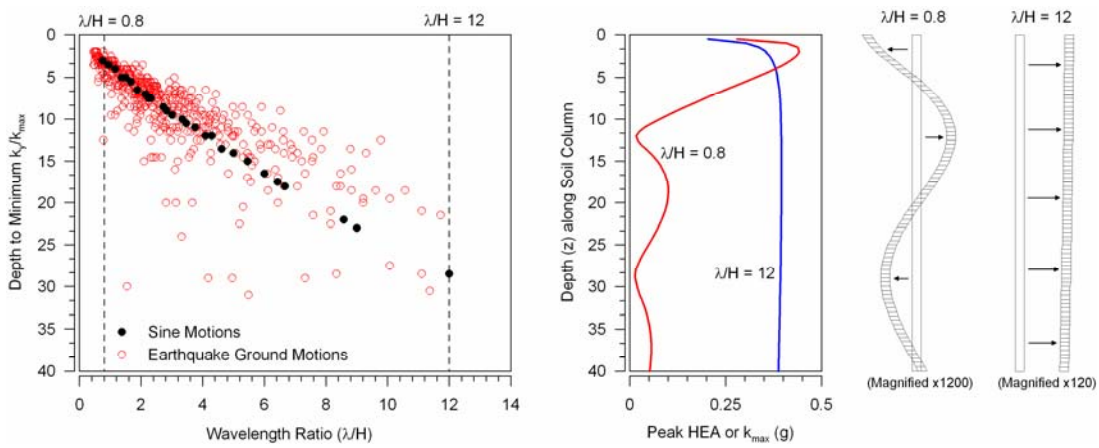


**Figure 5.** Variation of critical surface location and distribution of peak *HEA* for 1D soil columns

The relationship between the depth of minimum $k_y/k_{max}$ and the wavelength ratio for the earthquake and sine motions is shown in Figure 5. The overall trends for both types of motions are similar with the exception that the earthquake motion data displays significantly more scatter. This is attributed to the frequency-rich nature of the real ground motions and the limitations associated with characterizing the frequency content (and thus $\lambda/H$) using a single parameter ($f_m$). Figure 5 also shows $k_{max}$ as a function of depth at two different wavelength ratio conditions (sine motions only); the deformed shape of the soil column for these two conditions are also shown.

*2D Analysis Results*

The relationship between the surface descriptors ($h$, $V$, $D$, $\eta$) for the frictional-cohesive and purely cohesive cases is shown in Figure 6. Changes in the geometry of the failure mechanism are expressed in terms of the percent difference between the surface descriptor values for each best-fit surface obtained from the coupled analyses and those fit to the *FLAC* pseudostatic surface (non-associative flow rule, $\psi = 0^o$) (Fig. 3). By making this comparison, the pseudostatic and dynamic coupled analyses have consistent flow rule assumptions, and thus the observed changes in surface geometry shown in Figure 6 are due entirely to changes in dynamic response.

## Discussion and Conclusions

Overall, the dynamic response of a structure appears to have a significant effect on the geometry of the resulting failure mechanism, a trend that is supported by the results of the 1D and 2D analyses. The soil column analyses indicate that at lower $\lambda/H$ ratios shallower surfaces are more critical (more unstable) than at higher $\lambda/H$ ratios (Fig. 5). Likewise, the critical surfaces predicted by the fully-coupled 2D analyses display a similar trend with respect to the pseudostatic surface at lower $\lambda/H$ ratios (Fig. 6). Moreover, the 2D results display a non-linear relationship between dynamic response and failure mechanism geometry with the most significant changes occurring at $\lambda/H$ ratios between 1 and 4.

For both soil models considered, the asymptotic trend of the surface descriptors suggests that progressively lower frequency ground motions (higher $\lambda$) will have a reduced effect on the surface geometry. More specifically, this suggests that coupled surface obtained from the dynamic analyses tends to more closely match the geometry of the pseudostatic surface. Results from the soil column analyses

provide insight into this trend. When $\lambda/H$ is less than 1 (e.g. low $v_s$ and/or high $f_m$), the wavelength of the propagating motion through the model is less than $H$. Correspondingly, the response is more out-of-phase with movement within the model that varies in amplitude and phase. The net result is a distribution of accelerations (and inertial forces) that vary in magnitude throughout the model (as indicated by the deformed shape and $k_{max}$ distribution for $\lambda/H$ = 0.8 in Figure 5). Extending this to the 2D results and examining the trends in Figure 6 it appears that this occurs over a $\lambda/H$ range of 1 to 4 where the coupled surfaces tend to be smaller and shallower than the pseudostatic surface.

When $\lambda/H$ is greater than 1 (e.g. high $v_s$ and/or low $f_m$), the wavelength of the motion is greater than $H$, indicating that the response of the column is more in-phase and with a more uniform distribution of accelerations throughout the model. This is clearly indicated by the nearly constant value of $k_{max}$ with depth (for $\lambda/H$ = 12) as well as the corresponding monolithic movement implied by the deformed shape (Fig. 5). Consequently, the model is relatively non-compliant and unresponsive to dynamic loading, a condition where Newmark's rigid-block assumption is valid. The overall trends in Figure 6 show that for $\lambda/H$ ratios beyond 4 the geometry of the coupled surfaces approximates that of the pseudostatic surface. This result is reasonable considering that the "pseudostatic-stepping" method imparts a constant lateral downslope acceleration throughout the model which is similar to the distribution of accelerations associated with the dynamic response at larger $\lambda/H$ ratios.

Within the earthquake engineering community, practitioners and researchers alike have a shared interest in fully-coupled dynamic analyses citing the capability of modeling the coupled behavior of dynamic response and sliding response as its main advantage. Considering the results from this study it is clear that coupled analyses also offer another major advantage, principally the elimination of a priori assumptions and the development of failure mechanisms that are compatible with the dynamic response of the system.

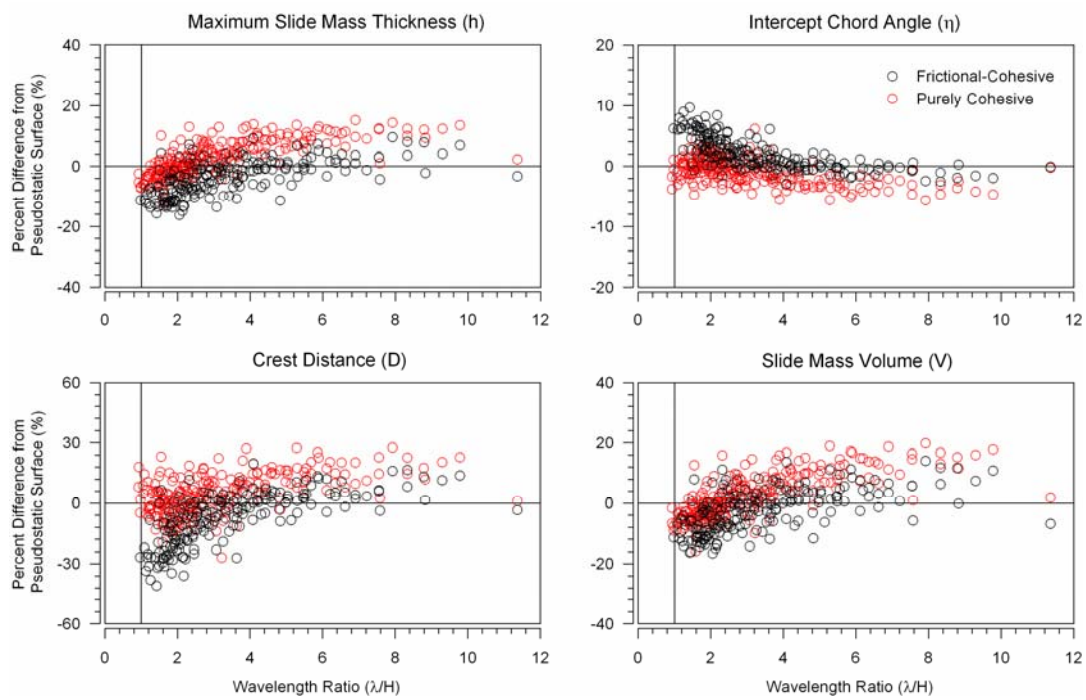


**Figure 6.** Changes in failure mechanism geometry as a function of $\lambda/H$

## ACCURACY OF DEFORMATION-BASED PROCEDURES

This phase of the research work aims to assess the accuracy and applicability of the analytical procedures used to predict seismically induced deformations by validating these methodologies against well-documented case histories. The principle goals of this research are to:

1. Systematically analyze a series of well documented earthquake-induced landslide case histories using a suite of deformation based analysis procedures. Analysis of each case history implemented within a Monte-Carlo framework to appropriately handle issues of data uncertainty.
2. Compare the actual "field" deformation measurements with those predicted by the analytical procedures and assess reliability and accuracy of each method using robust statistical analyses.

The following sections present a brief discussion of the accomplished tasks. The first section presents the software validation results of the dynamic analysis module of the *FLAC* software program. The second section presents a discussion of the Monte-Carlo approach adopted to handle issues of uncertainty and missing data for each case history. The third section briefly describes each of the deformation-based procedures selected for evaluation and the overall methodology of each procedure. The final section presents the results for a single well-documented case history using the approach discussed in the previous sections.

### Dynamic Response Validation of *FLAC*

The geotechnical software package *FLAC* (Fast Lagrangian Analysis of Continua) (Itasca 2005) was selected to perform the dynamic response analyses necessary for several deformation-based procedures. In practice, however, the earthquake engineering community is accustom to using traditional equivalent-linear codes such as *SHAKE91* (Idriss and Sun 1992, Schnabel et al. 1972) for 1D analyses and *QUAD4M* (Hudson et al. 1994) and *TELDYN* (Pyke 1992) for 2D analyses. The main motivation for using *FLAC* over these other codes is that the program is much more user-friendly and more versatile for constructing complex model geometries. However, despite these advantages, *FLAC* uses a new method to model strain-dependent modulus reduction ($G/G_{max}$) and damping ($\xi$).

The traditional linear-equivalent dynamic response codes listed above use an "iteration-based" computational scheme where the motion is passed through the model multiple times to approximate the hysteretic strain-dependent behavior of the soil. In *FLAC*, the hysteretic behavior is approximated more realistically using a "time-based" computational scheme where the modulus reduction and material damping are approximated in "each element at each time step" for a single passage of the motion through the model. Since *FLAC* uses such a different method to model the strain-dependent behavior of soil it was necessary to compare *FLAC* against the equivalent-linear codes. Comparisons were made for peak acceleration (PGA) and the horizontal equivalent acceleration (HEA) (Seed and Martin 1966, Chopra 1967)

Validation was performed for a 40 meter soil column and a 40 meter homogeneous slope similar to that shown in Figure1. The HEA time history for the 1D validation was obtained at a depth of 10 m below top of the soil column; the peak acceleration was recorded at the top of the column. The HEA time history for the 2D validation was determined for two slip surfaces using the methodology proposed by Chopra (1967); peak accelerations were recorded at the crest of the slope. A total of four shear wave velocity profiles were considered for each model. Each profile increases with depth and has an average value (calculated using Eqn. 2) ranging between 150 and 600 m/s (ICC 2006). The ground motions used in this validation are the same as those used for the fully-coupled analyses described above with the exception

that the as-recorded, un-scaled time histories were used. The peak acceleration of these motions ranges from approximately 0.01g to 1.5g.

The results of this validation are shown in Figures 9 and 10. On average, *TELDYN* yields $k_{max}$ values (i.e. peak of the HEA time history) that are 10% larger than FLAC. For the soil column analyses, *FLAC* and *SHAKE91* are in much closer agreement (< 5%). For both the 1D and 2D comparisons of the peak ground acceleration (PGA), *SHAKE91* and *TELDYN* are on average 10% greater than *FLAC*. This difference is most evident at PGA values greater than 0.5g which is outside the recommended range for equivalent-linear approximation. Based on these comparisons, it is clear that the agreement between *FLAC* and the equivalent-linear codes is very favorable.

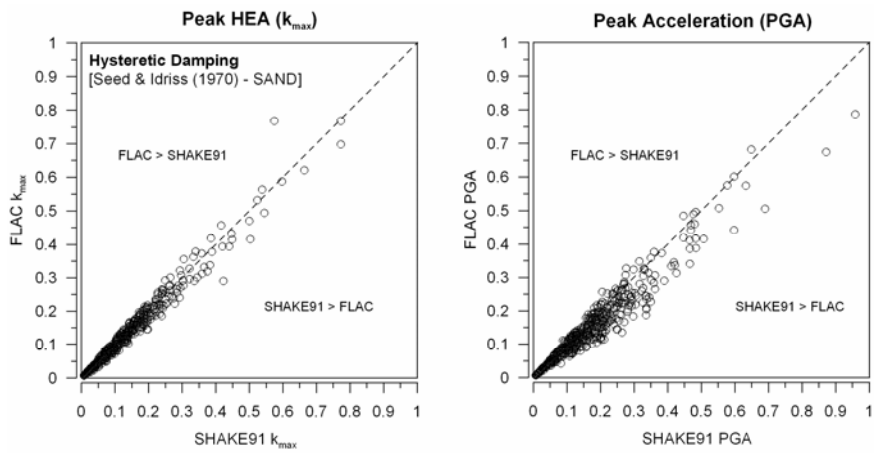


**Figure 9.** Soil column validation (equivalent-linear *SHAKE91* and hysteretic *FLAC*)

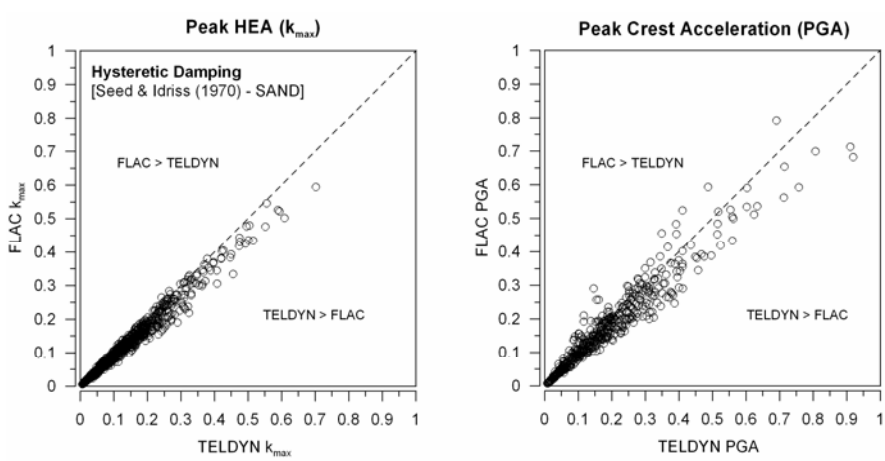


**Figure 10.** Slope model validation (equivalent-linear *TELDYN* and hysteretic *FLAC*)

Characterization of Seismic Resistance and Demand using Monte-Carlo

Previous research work for the first year of this project consisted of a comprehensive literature review that identified 13 well-documented case-histories of "coherent" (Keefer 1984) earthquake-induced landslides or earth structure movements. As a preliminary step, each of the case-histories were reviewed in detail and ranked according to the quality and quantity of their data. Even though these selected case histories

represent the most well documented studies found in the literature, the quantity of information reported varies greatly with some case histories having missing data.

To address these issues, a probabilistic Monte-Carlo approach was adopted in order to treat these uncertainties in a formal, consistent and quantitative manner. The Monte-Carlo method involves the computation of deterministic solutions for a large number of systematically generated realizations. The realizations are obtained from sampling probability distribution functions (PDF) characterizing the unknown or uncertain input variable(s). The output from such simulations is a collection of solutions (in this case deformation, $\delta$) that can be analyzed statistically. The Monte Carlo approach was implemented in the commercially available mathematical software MATLAB (MathWorks 2007).

The Monte-Carlo approach is a well validated approach that has become more popular tool for performing probabilistic static and seismic slope stability analyses (e.g. Mostyn & Li 1993, Kim 2001, El-Ramly et al. 2002) as well as in regional-scale analyses (e.g. Luzi et al. 2000). The following sections discuss the approach used to characterize the seismic resistance and seismic demand of each case history.

*Seismic Resistance* [programs STATPROP & PSLEM]

Overall, the selected case histories generally have a good to fair definition of the geotechnical soil properties (e.g. index and strength properties) of the soil materials. Typically, these soil properties were evaluated from of subsurface exploration and/or laboratory testing programs. However the quality of these programs as well as the quantity of information reported varies greatly. More common, is that most of the sites lack direct measurement of dynamic soil properties (e.g. shear wave velocity, $v_s$), which is a required input for the more sophisticated analysis procedures.

The parameters that are modeled as random variables are based on the data quality characteristics of the individual case history. The parameters that are most commonly modeled fall into two general categories: geotechnical soil properties [e.g. shear strength ($\phi$, $c$), unit weight ($\gamma$)] and dynamic soil properties [e.g. shear wave velocity ($v_s$)]. Other dynamic material properties such as modulus reduction ($G/G_{max}$) and damping ($\xi$) curves are not modeled probabilistically but were selected based on engineering judgment. Uncertainty in the depth to groundwater (if any) can also be modeled as a random variable. It should be noted that spatial-variation of soil properties is not modeled.

The STATPROP program performs two primary functions: generation of user-defined PDFs and random sampling of the PDFs. Although numerous studies have attempted to evaluate this, there is little substantial physical or theoretical evidence to suggest that a particular soil property always follows a specific analytical distribution. Thus, the selection of PDFs for modeling the variability of the input parameters is more a matter of convenience rather than being supported by hard data (Journel 1989). Typically, the soil property data for the case histories was obtained from small-scale subsurface investigations programs with limited sampling and testing which precludes the possibility of using a population of data to determine site-specific PDFs. As such, PDFs were assumed from the literature. Some of the more common distributions that are used include normal, log-normal and beta (e.g. Baecher and Christian 2003, Chowdhury 1984, Lumb 1966). Once the shape of the PDF is selected, the first and second moments (mean and variance) were defined. Typically, the mean was defined using the data provided in the case history or through the use of empirical correlations (e.g. Stark et al. 2005) whereas the variance (and standard deviation) of the PDF was defined based on published values of the coefficient of variation (COV) of the particular soil property of interest (e.g. Baecher and Christian 2003, Jones et al. 2002, Lacasse and Nadim 1996, Phoon and Kulhawy 1999). After the input parameter PDFs are defined, the STATPROP program randomly samples the distribution(s) using pseudo-random number generators built into *MATLAB*.

The output from the STATPROP program [geotechnical soil properties ($\phi$, $c$, $\gamma$)] is used as input into the program PSLEM that performs a limit-equilibrium pseudostatic analysis to calculate the seismic yield

coefficient ($k_y$). As defined by Newmark (1965), the seismic yield coefficient is a single parameter used to characterize the available resistance to earthquake shaking, or more specifically it represents the minimum acceleration required to bring the factor of safety against sliding to unity. All deformation-based procedures (with the exception of coupled method) require that $k_y$ be estimated. The PSLEM program uses an algorithm developed by Kim (2001) that is based on Spencer's limit-equilibrium formulation (Spencer 1967, 1973, 1978) to calculate the seismic yield coefficient directly without iterations. Spencer's method is recognized as one of the more accurate limit-equilibrium approaches (Duncan and Wright 1980) and due to its versatility has been recommended for usage in seismic hazard analyses (Blake et al. 2002). The computing efficiency of this algorithm is equivalent to traditional factor of safety evaluations and thus facilitates integration into a probabilistic Monte-Carlo framework (Kim and Sitar 2004).

*Seismic Demand* [program GENMOTION]

Due to the stochastic nature of earthquake ground motions, proper characterization of the input excitation is one of the most significant sources of uncertainty in dynamic response analyses. Thus, in terms of the input necessary for deformation-based procedures, ground motion characterization is more critical and can have a greater effect on the calculated deformations than the variability in soil properties (Kim 2001).

The most common approach to deterministically estimate site-specific ground motions at a particular site, involves the selection of several acceleration time histories that are subsequently matched to a design response spectrum obtained from an attenuation relationship. However, a small number of acceleration time histories matching a single design spectrum only represent a few possible realizations out of an infinite number of earthquake motion scenarios. With such a limited scope using such a technique will not sufficiently characterize the level of shaking experienced at the site. To overcome this, a method was developed that follows the same overall approach used in deterministic analyses but incorporates probabilistic components to handle the uncertainties in the earthquake motions. This approach fits into the Monte-Carlo framework adopted for this work and has the capability of creating a large database of motions with variability in intensity and frequency content that represent a realistic range of ground motion scenarios.

Although it is rare that an earthquake ground motion was recorded directly at the case history site, each of the case studies involve earthquake events that are generally well recorded and therefore make it possible to estimate site-specific motions with a reasonable degree of confidence. The method discussed below was developed to generate a database of motions that are realistic representations of what the each site might have experienced.

1. Find the acceleration recording stations that are closest to the case history site. Acceleration recording stations were selected on the following criteria: proximity to site, site-to-source azimuth, site geology and recording instrument location. Typically, recordings from between 3 and 6 stations were used.
2. Using the appropriate attenuation relationship determine the median, plus-one standard deviation ($+1\sigma$) and minus-one ($-1\sigma$) standard deviation target response spectra corresponding to the site-source distance of the case history.
3. Model the standard deviation ($\sigma$) of the target spectra as a random variable (the peak of the probability distribution corresponds to the median spectra).
4. Randomly select a target spectrum from the probability distribution and randomly select one of the ground motion recordings (from step 1).
5. Match the selected acceleration time history to the selected target spectra using a spectral matching algorithm (Basu & Gupta 1998, Mukherjee and Gupta 2002) to obtain the spectra-compatible

acceleration time history. Repeat until the desired number of ground motion realizations are obtained.

The spectral-matching algorithm is an iterative, wavelet-based approach employing the modified Littlewood-Paley (L-P) basis function to decompose a recorded acceleration time history. Decomposition is achieved through a wavelet analysis that separates the recorded ground motion into a finite number of time histories with energy in non-overlapping frequency bands. The time histories in each of these bands are iteratively scaled to match the target response spectra. Mukherjee and Gupta (2002) have demonstrated that the spectrally-matched time histories preserve the non-stationary characteristics of the parent motions very well. In addition, this wavelet-based approach is more direct and realistic than other available procedures that model the phase characteristics of the motion through the use of Fourier spectra and power spectral density functions (e.g. Kim 2001).

Deformation-Based Procedures

The current state of the practice for assessing seismically-induced deformations in slopes relies on one or more procedures that generally fall into three categories:

1. *Rigid-block procedures*, which neglect the dynamic response;
2. *Decoupled procedures*, which account for dynamic response, but "decouple" it from the sliding response;
3. *Coupled procedures*, which "couple" the dynamic response and sliding response as a single behavior.

A further distinction within these three categories is how the procedure is implemented, either deterministically or analytically. This distinction is only applicable to the first two categories listed above. All deterministic methods are equation or chart-based in their application and thus very easy to program and automate. The analytical methods are more involved requiring direct computation of the dynamic response and/or the sliding response. In total, 15 deformation-based procedures were evaluated. These methods are listed in Table 2.

**Table 2** – List of deformation-based procedures selected to evaluate

**Rigid-Block Methods:**

Deterministic:

1. Ambraseys & Menu (1988) [AM1988]
2. Franklin & Chang (1977) [FC1977]
3. Hynes-Griffin & Franklin (1984) [HGF1984]
4. Jibson (1994) [JB1994]
5. Newmark (1965) [NM1965]
6. Richards & Elms (1979) [RE1979]
7. Sarma (1975) [SM1975]
8. Whitman & Liao (1984) [WL1984]
9. Yegian (1991) [YG1991]

Analytical:

10. "Double-Integration" analysis [SLIP]

**Decoupled Methods:**

Deterministic:

11. Hynes-Griffin & Franklin (1984) [HGFDEC1984]
12. Makdisi & Seed (1978) MSDEC1978]
13. Bray & Rathje (1998) [BRDEC1998]

Analytical:

14. 1D decoupled analysis [1DYNRESP; SLIP]
15. 2D decoupled analysis [2DYNRESP; SLIP]

**Coupled Methods:**

Analytical:

16. 2D fully-coupled nonlinear analysis [COUPFLAC]

As mentioned earlier each of these methods was implemented as a series of programs written in *MATLAB*. The name of each program (shown in brackets) is listed after each method displayed in Table 2 (e.g. [AM1988]). A detailed description of the background and development of each of these methods is excluded for brevity. However, the relevant references corresponding to each method are listed in Appendix A.

*Method Implementation*

The distinctions made between the three categories of deformation-based methods are related to the simplifying assumptions proposed during their original development. These assumptions focus mainly on the manner in which the mechanism of seismically-induced deformation is modeled; some methods being more realistic than others. As such, the level of sophistication associated with each deformation method necessarily leads to different procedures required for their implementation. The following discussion presents the step-by-step procedure associated with each category of deformation-based procedures shown in Table 1. For clarity, it is presented in terms of individual *MATLAB* programs written for each component of the overall procedure.

Common to the implementation all rigid-block and decoupled procedures (deterministic or analytical) are the following two steps:

1. Characterization of seismic demand (in the form of representative base input acceleration time histories or a collection of peak accelerations (PGA) from those time histories) [program GENMOTION]. Typically a database of 100 to 200 ground motions was generated.
2. Characterization of seismic resistance through a limit-equilibrium pseudostatic analysis to calculate the seismic yield coefficient ($k_y$) [programs STATPROP then PSLEM]. Typically a collection of 1000 to 5000 realizations were generated.

The output from GENMOTION and PSLEM are used for the subsequent analyses of the rigid-block and decoupled procedures and are illustrated at the top of the flow charts shown in Figures 11 through 8. For the rigid-block procedures, the deformation analysis is performed using either deterministic equations (Figure 11) or by means of analytical numerical "double-integration" [program SLIP] (Figure 12).

Unlike the rigid-block procedures, decoupled analyses require the following two-step procedure: 1.) perform a dynamic response analysis to characterize the seismic demand (HEA) on the slide mass and 2.) use the HEA time history as input into the deformation analyses. For the deterministic decoupled procedures, dynamic response and deformations are determined from chart-based solutions [programs BRDEC1998, HGFDEC1984] (Figure 7). An exception to this is Makdisi and Seed (1978) decoupled method [program MSDEC1978] that requires a 2D dynamic response analysis [program 2DYNRESP] to determine the peak acceleration recorded at the crest of the model (Figure 7). Using this value, a chart is consulted to obtain peak HEA (or $k_{max}$) and an additional chart is then used to calculate deformations. For the analytical decoupled procedure, dynamic response is evaluated for 1D and 2D conditions using the software package *FLAC* and implemented through the programs 1DYNRESP and 2DYNRESP (Figure 8). Both programs implement an algorithm to calculate the horizontal equivalent acceleration experienced by the slide mass (Seed and Martin 1966, Chopra 1967). Using the HEA time histories, deformations are calculated through numerical "double-integration" [program SLIP].

For the non-linear, fully-coupled analyses, the output from the program STATPROP (both the geotechnical and dynamic soil properties) are assigned directly to the 2D model constructed in *FLAC*. The motions obtained from GENMOTION then propagated through the model. For this category of analyses, the dynamic response and sliding response occur simultaneously and the failure surface evolves naturally instead of being prescribed by the results of a LEM pseudostatic analysis. The procedure for these fully-coupled analyses is shown in Figure 15.

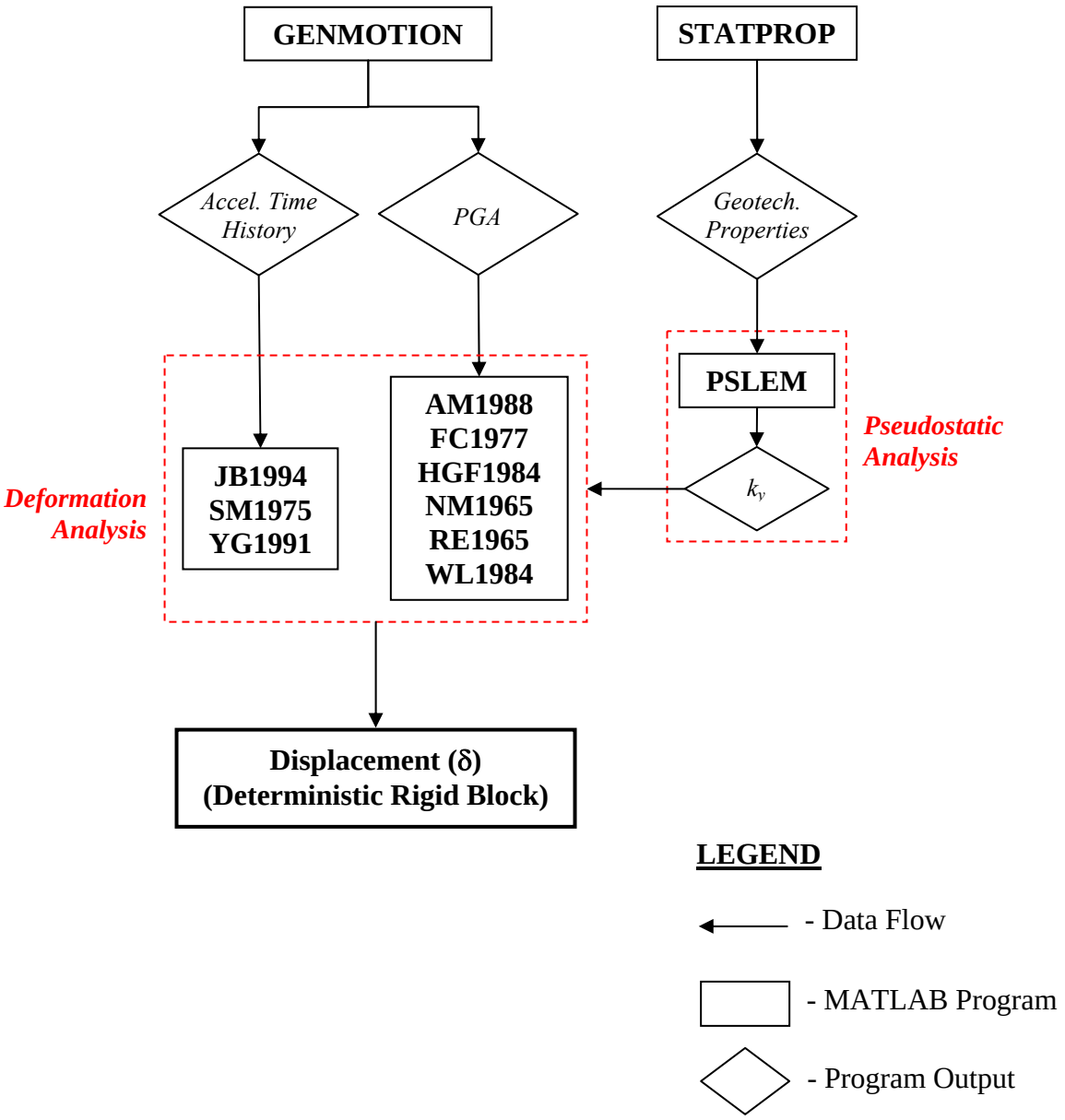


**Figure 11.** Program implementation and data flow for deterministic rigid-block methodology

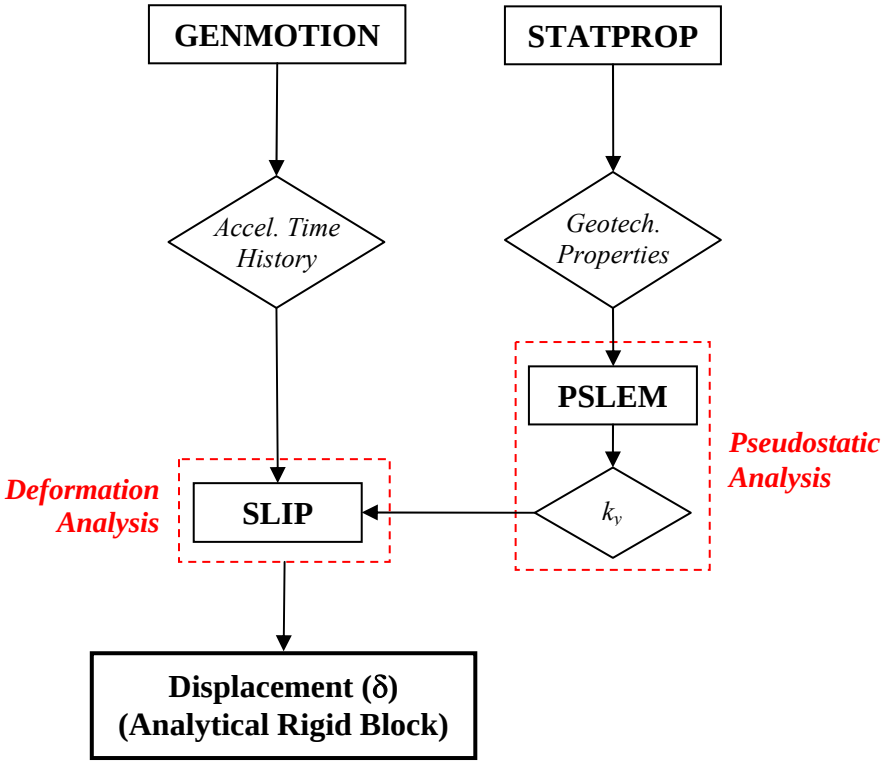


**Figure 12.** Program implementation and data flow for analytical rigid-block methodology

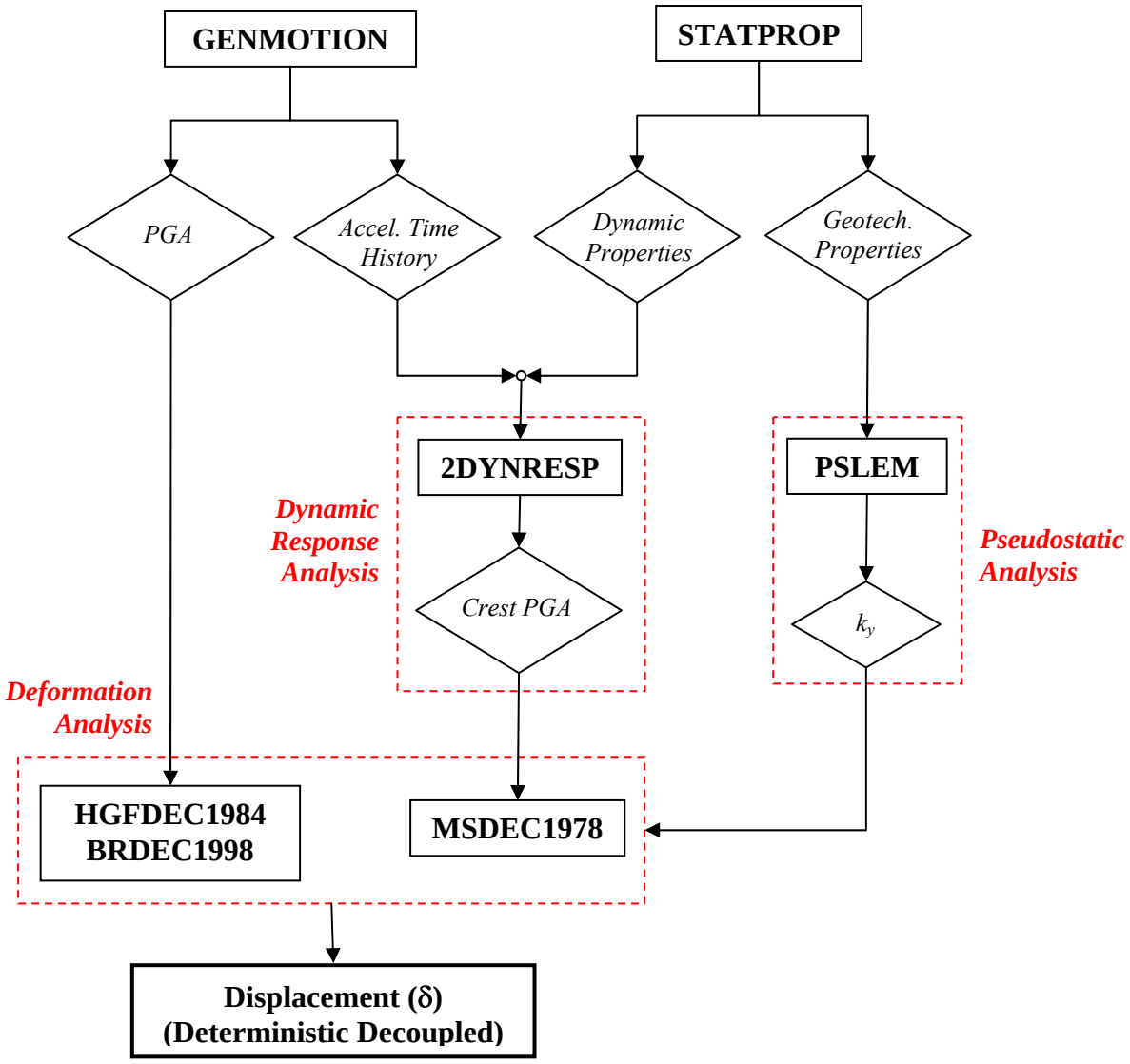


**Figure 13.** Program implementation and data flow for deterministic decoupled methodology

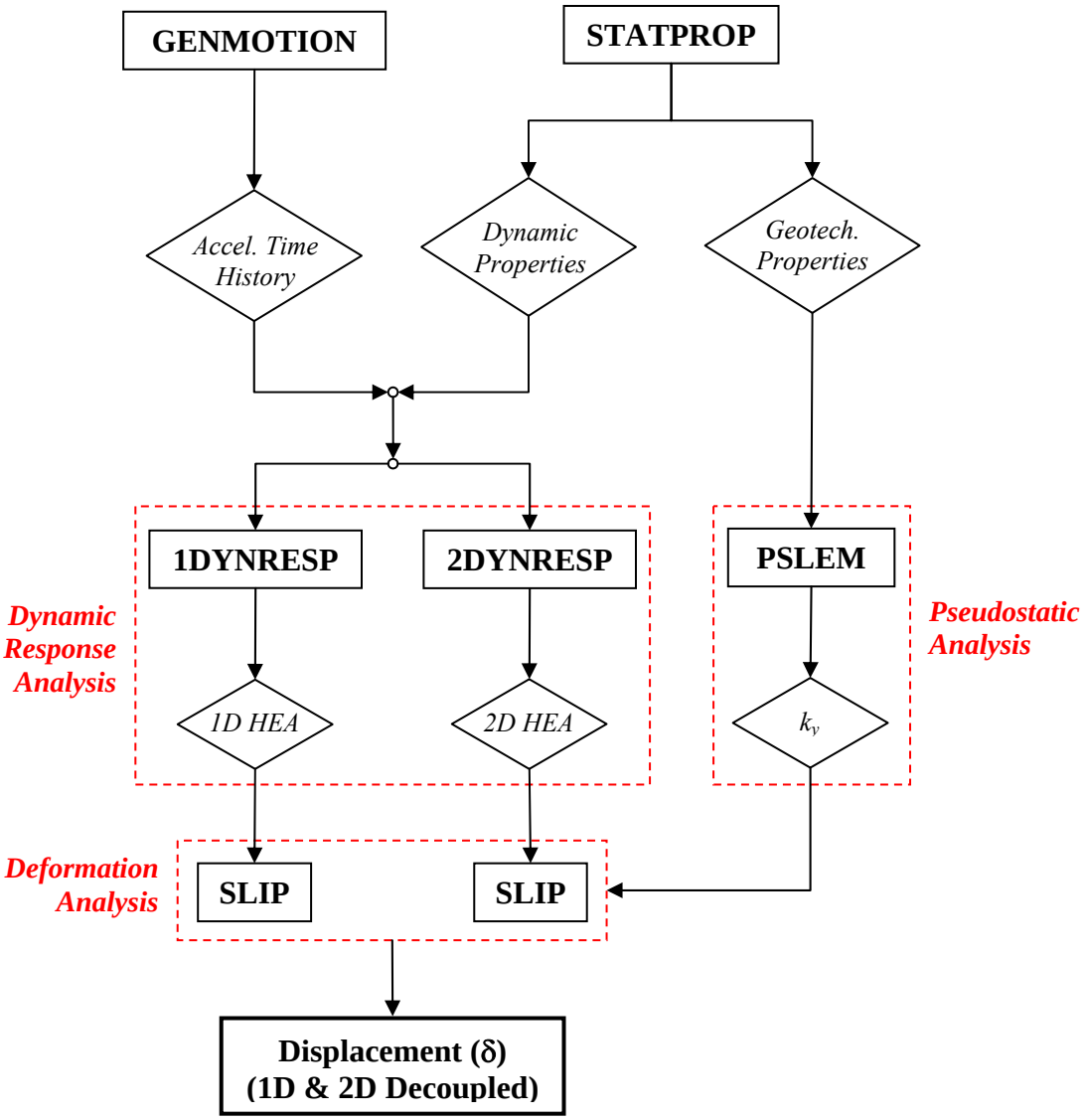


**Figure 14.** Program implementation and data flow for analytical decoupled methodology

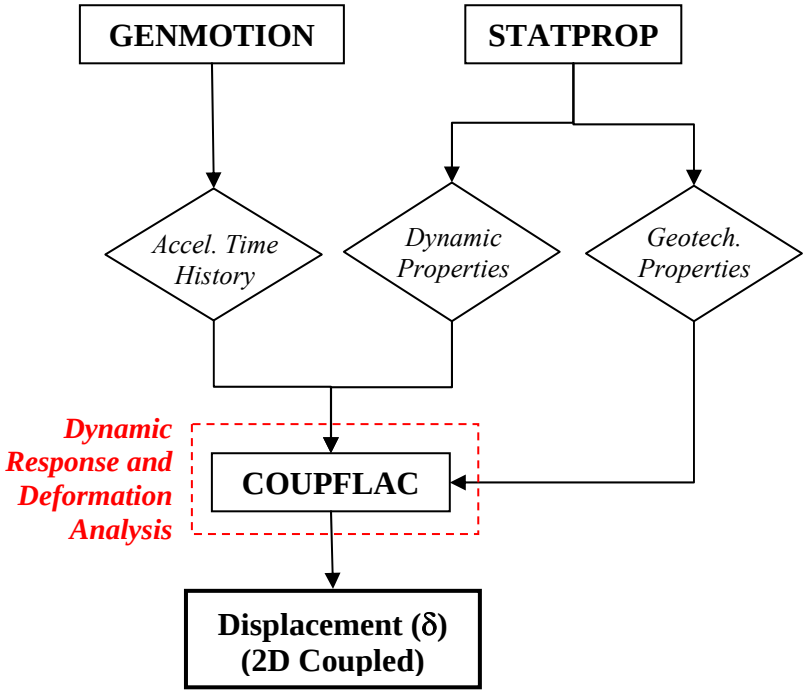


**Figure 15.** Program implementation and data flow for nonlinear fully-coupled methodology

Case History Analysis

The Ditullio landslide is located in the Santa Cruz Mountains of California and was triggered by the 1989 Loma Prieta earthquake. Ditullio landslide is characterized as a single, reactivated, deep, coherent rock slump or rock block slide and displayed a progressive, rotational movement (Keefer 1984). Ditullio landslide is roughly 18 m thick at its deepest point and roughly 100-120 m long by 60-70 m wide with an estimated volume of 54,500 $m^3$. Ditullio landslide is a reactivated landslide located within a very large ancient landslide complex in the Santa Cruz Mountains. The following discussion summarizes the subsurface conditions at the landslide site as well as the laboratory testing performed by Cole et al. (1991).

*Subsurface Conditions & Soil Properties*

The landslide deposits consist of plastic silty clay to clayey/silty sand colluvium (typically 2 m thick) followed by zone of highly-weathered, oxidized and fractured decomposed bedrock regolith. The regolith consists of angular gravel to boulder-sized siltstone and sandstone rock fragments with varying amounts of clayey silt to silty sand matrix. A well-developed shear surface marks the transition from the over-lying, oxidized regolith material to more competent underlying bedrock. The shear zone separating the two units is a moist, clayey silt to silt with a soft to firm consistency and medium to high plasticity (typically 1 to 10 cm thick). Overall, the transition from overlying, oxidized regolith to unoxidized, closely fractured bedrock is gradual over 3 m, however, this transition is less gradual and more pronounced in the vicinity of the shear zone. The bedrock is

consists of Tertiary age, unoxidized and closely fractured, fine to medium grained sandstone and siltstone. Cole et al. (1991) classified the rock as being part of the San Lorenzo formation. No evidence of a ground water table was found.

One large-diameter boring was drilled into Ditullio landslide. The boring, which was located about 40 m downslope from the landslide headscarp, was drilled and logged to a depth of 22.5 m. The borehole had a diameter that was large enough for personnel to be lowered downhole permitting visual inspection and logging of the subsurface conditions. In-situ field testing was not performed during the subsurface investigation of this landslide with the exception of several torvane and pocket penetrometer readings taken during downhole inspection. The subsurface investigation did not evaluate the shear wave velocity of the bedrock regolith. Several disturbed grab samples were taken at various depths to evaluate the index properties of the material (i.e. USCS classification, dry density, moisture content, and Atterberg limits). Dry density tests indicated that the moist unit weight ($\gamma$) of the bedrock regolith material ranged from 17.4 to 19.6 kN/m$^3$. Two oriented, undisturbed samples were taken of the shear zone (at the same location, 18 m depth) and two types of direct shear tests were performed to obtain peak and residual strength parameters. Index tests performed on the fine-grained materials comprising the shear zone indicated a liquid limit (LL) of 36, plastic limit (PL) of 25, a plasticity index of 9 and a clay fraction of 18%. Peak strength parameters were obtained for both samples and residual strength parameters were obtained for only one sample. The test results were analyzed to obtain lower bound, upper bound and best-fit values that were subsequently used in their own stability and deformation analyses. As well as providing friction angle and cohesion values, Cole et al. (1991) also included the direct shear test results in terms of the normal stress and peak and residual shear stress values. However, instead of using the results report by Cole et al. (1991), it was decided to perform a regression analysis to re-evaluate the friction angle and cohesion values. Based on this re-analysis, the peak shear strengths were calculated as $\phi$ = 26.8$^o$, $c$ = 35.3 kPa and $\phi$ = 47.8$^o$ and $c$ = 2.3 kPa. The residual strength parameters were calculated as $\phi$ = 28.6$^o$, $c$ = 9.55 kPa.

*Deformation*

The headscarp and right flank areas of the landslide showed signs of distress characterized by arcuate, en echelon and parallel ground fissures and cracks. The left flank showed no signs of deformation. Individual cracks in the headscarp area indicated between 30 and 60 cm of downslope movement (extension) and approximately 30 cm of vertical drop. Using these two components of movement, the resultant displacement was calculated to be between 42 and 67 cm.

*Ground Motion Characterization*

As the first step of ground motion characterization for the Ditullio landslide, it was necessary to gather a series of recorded time histories to be used as input into the GENMOTION program. Selection of the ground motion time histories was based on the following criteria: recording station location, relative source-to-station azimuth, and site geology.

For the first criterion, only stations that were the closest to the landslide site were selected as these are more likely to represent the ground shaking experienced at the landslide. Stations within a 20 km radius of the landslide site were considered. The stations meeting this condition were further refined according to source-to-landslide azimuth. By introducing this criterion into the selection process possible variations in ground motions due to rupture-directivity effects are indirectly accounted for. Since the landslide is located within the forward-rupture directivity region at the northwest portion of the rupture plane, only stations that had a similar azimuth as the landslide site were selected. Based on the first two criteria the selections include: Branciforte Drive (BRN), Los Gatos Presentation Center (LGP), Lexington Dam (LEX), and Saratoga – Aloha Ave. (STG).

For the final criterion, each of the selected time histories listed above fall under the general category of "rock" sites according to the classification scheme proposed by Bray and Rodriquez-Marek (1997). The "B" and "C" categories shown in Table 1 indicate that the recording stations are located over "rock" or "weathered soft rock/shallow stiff soil," respectively. These classifications are consistent with the overall subsurface

conditions at the Ditullio landslide. Moreover, the site geology at the BRN, STG and LGP stations is reported as Tertiary or Quaternary age which is also consistent with the deposits at the landslide site. The LEX station, however, overlies older Cretaceous and Jurassic age deposits of the Franciscan formation. Despite these differences, the use of the LEX station recording is justified because of its close proximity to the landslide (< 10 km). Since these strong motion recordings were obtained from stations classified as being a "rock" sites, deconvolution procedures were not required. A summary of the selected ground motion recordings are shown in Table 3.

**Table 1.** Strong motion stations near Ditullio landslide that recorded the 1989 Loma Prieta earthquake

| Station | Identification | Site Classification [a] | $r$ [b] |
|---|---|---|---|
| Los Gatos Presentation Center (LGP) | UCSC 16 | C | 3.88 |
| Lexington Dam (LEX) | CDMG 57180 | B | 5.02 |
| Saratoga – Aloha Ave. (STG) | CDMG 58065 | C | 8.50 |
| Branciforte Drive (BRN) | UCSC 13 | B | 10.72 |
| San Jose – Santa Teresa Hills (SJT) | CDMG 57563 | B | 14.69 |

Note: [a] Classification scheme from Rodriquez-Marek et al. (2001)
[b] Closest distance to 1989 Loma Prieta fault rupture plane.

These five ground motion recordings were used as input into the GENMOTION program for response spectra matching. The response spectra used for matching was obtained from the Abrahamson and Silva (1997) attenuation relationship for shallow crustal earthquakes. As outlined before, the GENMOTION program uses a wavelet-based algorithm to match a randomly selected target spectrum. This program was used to develop a database of 100 spectra-compatible ground motions that are a realistic representation of the level of shaking experienced at the landslide site. An example output from the GENMOTION program is shown in Figure 16.

*Uncertain Soil Properties*

Considering that the Ditullio landslide is a reactivated landslide located within a very large ancient landslide complex, it was assumed that the shear strength parameters were near their residual strength values at the time of the earthquake. This assumption is appropriate for old, coherent landslides with pre-existing rupture surfaces. By using residual strength conditions, it was assumed that the cohesive component of strength ($c$) was negligible in comparison to the frictional shear resistance ($\phi$) (Stark et al. 2005). Thus, the pre-existing landslide surface was assumed to mobilize frictional strength only. The mean values of frictional strength for the soil materials was based on the published residual strength values in Cole et al. 1991 as well as an empirical correlation. The empirical correlation developed by Stark et al. 2005, relates the residual friction angle ($\phi_{residual}$) (as a function of effective stress) to the liquid limit and the percent clay fraction. Based on the index properties of the shear zone materials, a residual strength of 28$^o$ was calculated using this correlation and compares favorably with the laboratory derived value of 28.6$^o$ presented above. Based on these strength properties and a published coefficient of variation (COV) of 20% (Baecher and Christian 2003), the STATPROP program was used to generate 1000 values $\phi_{residual}$ from a normal distribution with a mean defined at of 28$^o$. Considering the relatively narrow range of reported unit weight values it was deemed unnecessary to model this parameter as a random variable, as such an average value of 18.5 kN/m$^3$ was used.

As stated above, the dynamic soil properties were not evaluated at this landslide. As such, it was necessary to use an empirical correlation to establish the likely range of shear wave velocity values landslide materials. Wills and Silva (1998) correlated the average shear wave velocity to the type and age of geologic units in California. Using this correlation, an average shear wave velocity of 420 m/s (with a standard deviation of 110 m/s) was considered to be representative of the Tertiary age bedrock at the landslide site. These statistical quantities were then used in conjunction with Eqn. 1 (Seed and Idriss 1970) to generate a suite of shear wave velocity profiles

representing a realistic range of the soil conditions at the site. Figure 17 shows the distribution of simulated friction angles and shear wave velocity profiles used for the Monte Carlo simulation.

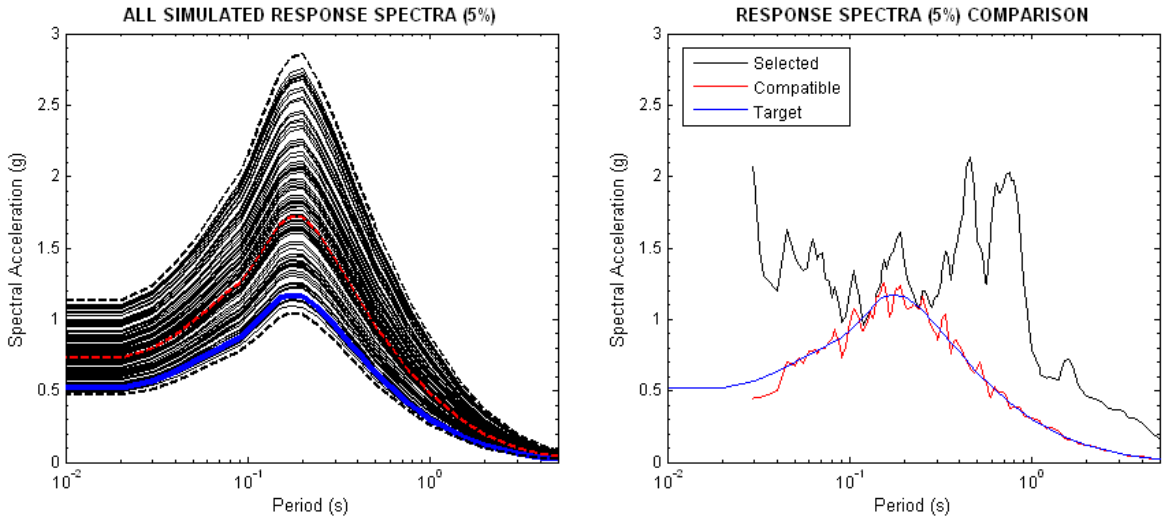


**Figure 16.** Example output from the GENMOTION program

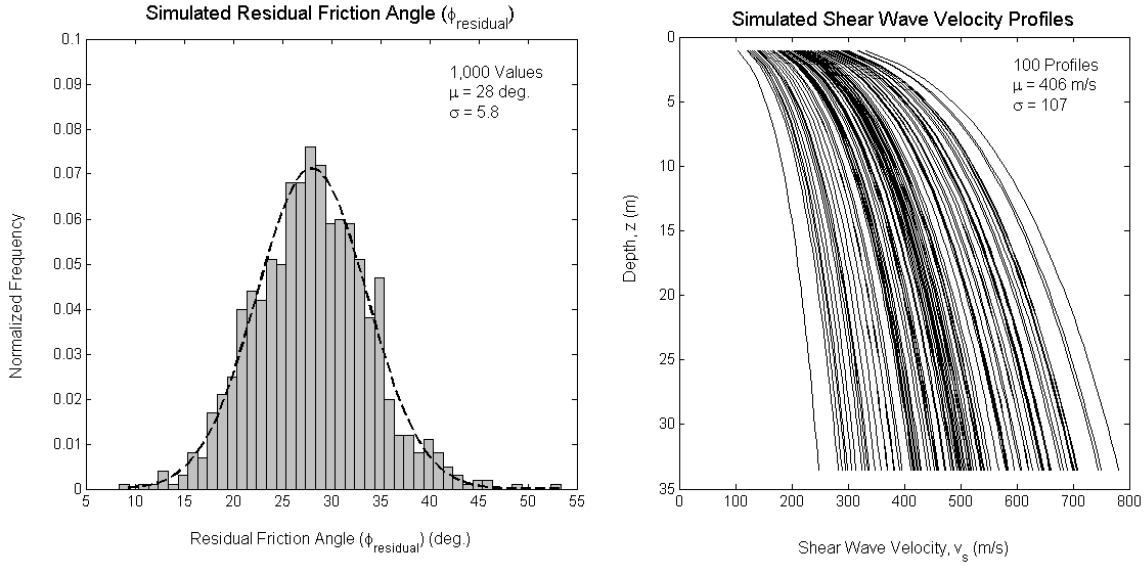


**Figure 17.** Simulated values of residual friction angle (fresidual) and shear wave velocity profiles (output from the STATPROP program)

*Deformation-Based Analyses*

The deformation response of the Ditullio landslide was analyzed with all rigid-block methods (deterministic and analytical) as well as by the 1D decoupled procedure. The results are shown in Figure 18. The bar chart for each method shown in Figure 18 represents the distribution of deformations calculated for the landslide. The

two dotted lines indicate the range of actual displacements measure at the Ditullio landslide. All deformations are in centimeters (cm).

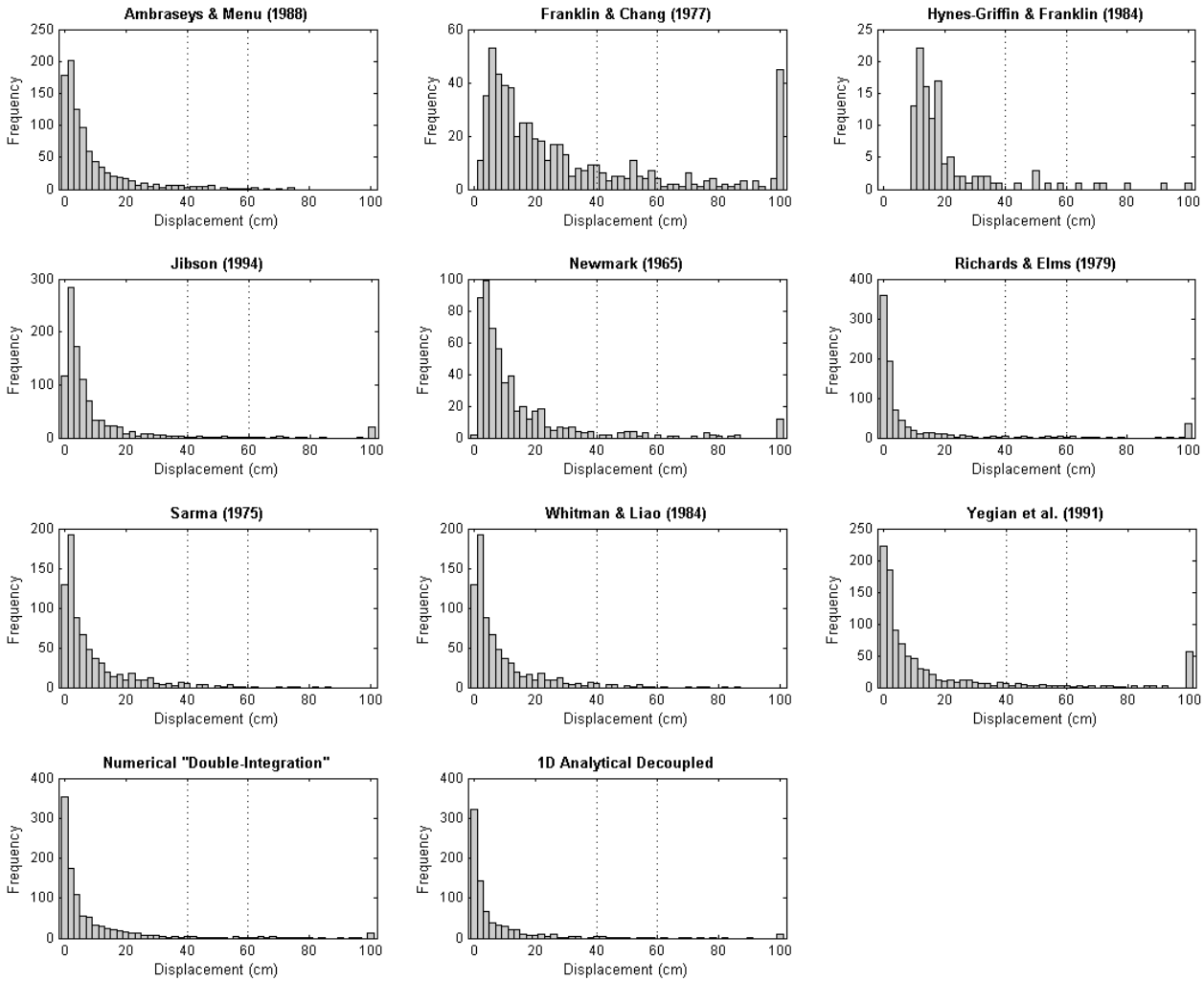


**Figure 18.** Results comparing predicted and actual deformations for the Ditullio landslide

Discussion and Conclusions

A comprehensive framework has been developed to back-analyze the seismically induced landslide case histories. Noteworthy is the treatment of uncertainty in the input parameters, which can have a significant influence on the results of the deformation analyses. The Monte Carlo-based approach used in this work addresses in a quantifiable manner uncertainly in both seismic demand (e.g. earthquake ground motion, local shaking at site) and resistance (e.g. subsurface properties and characteristics). Although developed specifically for this work, the back-analysis framework and its treatment of uncertainty is applicable to other similar case history- based studies. For brevity, a detailed presentation of results has been provided for only the Ditullio landslide; however, these results are generally consistent with those of the other case studies (detailed in previous report to the USGS, Award No. 04HQGR0165). The systematic under prediction of the deformations in the case of the Ditullio landslide are likely related to two factors: use of static soil properties for dynamic analysis, and limitations to the deformation methodologies themselves, which only account for localized shearing deformation. Under seismic loading, actual slopes permanently displace in response to this and other mechanisms such as distributed internal straining and seismic compression of soil.

Project Publications

Strenk, P. M. and Wartman, J. (2008) "Validity of the Pseudostatic Surface Assumption for Evaluating Seismically-Induced Deformation in Slopes," *Proc., First International FLAC/DEM Symposium on Numerical Modeling*, Minneapolis, August 2008.

Two papers related to the second phase of the research are currently in preparation, with anticipated submission to the journal Engineering Geology

**REFERENCES**


Abrahamson, N.A. and Silva, W.J. (1997). "Empirical response spectral attenuation relations for shallow crustal earthquakes." *Seism. Res. Letters*, 68(1), 94-127.

Baecher, G. B., and Christian, J. T. (2003). *Reliability and statistics in geotechnical engineering*, Wiley, New York.

Basu, B. and Gupta, V.K. (1998). "Seismic response of SDOF systems by wavelet modeling of nonstationary processes." *J. Engrg. Mech.* 124(10), 1142-1150.

Blake, T. F., Hollingsworth, R. A., and Stewart, J. P., eds. (2002). "Recommended procedures for implementation of DMG Special Publication 117 guidelines for analyzing and mitigating landslide hazards in California." South. Calif. Earthq. Ctr, Univ. of South. California, Los Angeles, Calif.

Chen, W.F. (1975). *Limit analysis and soil plasticity*. Elsevier, Amsterdam.

Chopra, A.K. (1967). "Earthquake response of earth dams." *J. Soil Mech. and Found. Div.* 90(SM2): 65-81.

Chowdhury, R.N. (1984). "Recent developments in landslide studies: probabilistic methods – state of the art report." *Proc. 4th Internat. Symp. On Landslides*, Toronto, Vol. 1, 209-228.

Cole, W.F., Marcum, D.R., Shires, P.O., and Clark, B.R. (1991). "Investigation of landsliding triggered by the Loma Prieta earthquake and evaluation of analysis methods." William Cotton and Associates, Los Gatos, California.

Drescher, A. & Detournay. E. 1993. "Limit load in translational failure mechanisms for associative and non-associative materials." *Géotechnique* 43(3), 443-456.

Duncan, J. M., and Wright, S. G. (1980). "The accuracy of equilibrium methods of slope stability analysis." *Engrg. Geol*., 16, 5–17.

El-Ramly, H., Morgenstern, N.R. and Cruden, D.M. (2002). "Probabilistic slope stability analysis for practice." *Canad. Geotech. J.* 39(3), 665-683.

Griffiths, D.V. & Kidger, D.J. (1995). "Enhanced visualization of failure mechanisms by finite elements." *Comp. and Struct.* 55(2), 265-268.

Hudson, M., Idriss, I. M., and Beikae, M. (1994). *QUAD4M: A computer program to evaluate the seismic response of soil structures using finite element procedures and incorporating a compliant base*. Center for Geotechnical Modeling, Dept. of Civil and Environ. Engrg., Univ. of California, Davis, Calif.

Idriss, I. M. and Sun, J.L. (1992). *User's manual for SHAKE91*. Center for Geotech. Modeling, Dept. of Civil and Environ. Engrg, Univ. of California, Davis, California.

International Code Council (ICC). 2006. *International Building Code (IBC)*. Country Club Hills: The International Code Council.

Itasca Consulting Group. (2005). *FLAC – Fast Lagrangian Analysis of Continua, Version 5 User's Manual*. Minneapolis, Minn.

Jones, A.L., Kramer, S.L. and Arduino, P. (2002). *Estimation of uncertainty in geotechnical properties for performance-based earthquake engineering*. PEER Report 2002/16, Pacif. Earthq. Engrg. Res. Ctr., Univ. of California, Berkeley, Calif.

Journel, A.G. (1989). *Fundamentals of Geostatistics in Five Lessons*, American Geophysical Union.

Keefer, D. K. (1984). "Landslides caused by earthquakes." *Geol. Soc. of Amer. Bull*., 95(4), 406-421.

Kim, J. (2001) "Probabilistic approach to evaluation of earthquake induced permanent deformation of slopes." PhD dissertation, Dept. of Civil and Environ. Engrg., Univ. of California, Berkeley, Calif.

Kim, J. and Sitar, N. (2004). "Direct estimation of yield acceleration in slope stability analyses." *J. Geotech. and Geoenviron. Engrg*., 130(1), 111-115.

Kramer, S.L. and Smith, M.W. (1997). "Modified Newmark model for seismic displacements of compliant slopes." *J. Geotech. and Geoenviron. Engrg*., 123(7), 635-644.

Lacasse, S. and Nadim, F. (1996). "Uncertainties in characterizing soil properties." *Uncertainty in the geologic environment*, C. D. Shackelford, P. P. Nelson, and M. J. S. Roth, eds., Geotechnical Special Publications No. 58, ASCE, Madison, Wis., 326–340.

Lumb, P. (1966). "The variability of natural soils." *Cand. Geotech. J*. 3(2), 74-97.

Luzi, L., Pergalani, F. and Terlien M.T.J. (2000). "Slope vulnerability to earthquakes at subregional scale, using probabilistic techniques and geographic information systems." *Engrg. Geol*., 58, 313–336.

Makdisi, F. I. and Seed, H. B. (1978) "Simplified procedure for estimating dam and embankment earthquake-induced deformations." *J. of Geotech Engrg.,*104(7), 1427-1434.

Mathworks. 2007. *MATLAB 7 – Programming.* The MathWorks, Inc., Natick, Mass.

Mostyn, G.R. and Li, K.S. (1993). "Probabilistic slope analysis – state at play." *Probabilistic methods in geotechnical engineering*, Li, K.S. and Lo, S-C, R. eds., A.A. Balkema, Rotterdam, 89-109.

Mukherjee, S. and Gupta, V.K. (2002). "Wavelet-based generation of spectrum-compatible time histories." *Soil Dyn. And Earthq. Engrg.* 22, 799-804.

Newmark, N. M. (1965) "Effects of earthquakes on dams and embankments." *Géotechnique*, 15(2), 139-160.

Phoon, K. K., and Kulhawy, F. H. (1999). "Characterization of geotechnical variability." *Can. Geotech. J.*, 36(4), 612–624.

Pyke, R.M. (1992). *TELDYN: user's manual.* TAGAsoft Limited, Lafayette, Calif.

Rathje, E.M., Abrahamson, N.A. & Bray, J.D. (1998). Simplified frequency content estimates of earthquake ground motions. *J. Geotech. and Geoenviron. Engrg*., 124(2), 150-159.

Refice, A. and Capolongo, D. (2002). "Probabilistic modeling of uncertainties in earthquake-induced landslide hazard assessment." *Comp. & Geoscien*., 28, 735–749.

Rodriquez-Marek, A., Bray, J.D., and Ambrahamson, N.A. (2001). “An empirical geotechnical seismic site response procedure.” *Earthq. Spectra*, 17(1), 65-87.

Schnabel, P.B., J. Lysmer and H.B. Seed (1972). *SHAKE: a computer program for earthquake response analysis of horizontally layered sites.* Earthq. Engrg. Res. Ctr. UBC/EERC 72-12, Univ. of California, Berkeley, Calif.

Seed, H.B. & Idriss, I.M. (1970). *Soil moduli and damping factors for dynamic response analyses*. Report EERC 70-10, Earthq. Engrg. Res. Ctr., Univ. of California, Berkeley, Calif.

Seed, H.B. and Martin, G.R. (1966). “The seismic coefficient in earth dam design.” *J. Soil Mech. and Found. Div.*, 92(SM3), 25-58.

Shukha, R. & Baker, R. (2003). Mesh geometry effects on slope stability calculation by FLAC strength reduction method – linear and non-linear failure criteria. In Brummer et al. (eds), *FLAC and Num. Mode. in Geomech. – 2003; Proc. 3rd Int. FLAC Symp., Ontario, 21-24 October 2003*. Lisse, Balkema.

Spencer, E. (1967). “A method of analysis of the stability of embankments assuming parallel inter-slice forces.” *Géotechnique*, vol. 17, 11–26.

Spencer, E. (1973). “Thrust line criterion in embankment stability analysis.” *Géotechnique*, 23(1), 85-100.

Spencer, E. (1978). "Earth slopes subject to lateral acceleration." *J. Geotech. Engrg. Div.,*104(GT12), 1489-1500.

Stark, T.D, Choi, H. and McCone, S. (2005). “Drained shear strength parameters for analysis of landslides.” *J. Geotech. and Geoenviron. Engrg*., 131(5), 575-588.

Vermeer, P.A. and de Borst, R. (1984). “Non-associated plasticity for soils, concrete and rock.” *Heron*, 29(3), 1-64.

Wills, C.J. and Silva, W.J. (1998). Shear-wave velocity characteristics of geologic units in California.” *Earthq. Spectra*, 14(3), 533-556.

## APPENDIX A
## Relevant References for Deformation-Based Procedures

### Deterministic rigid-block methods


Ambraseys, N. N. & Menu, J. M. (1988). "Earthquake-induced ground displacements." *Earthq. Engng Struct. Dyn.,* 16(7), 985-1006.

Cai, Z. & Bathurst, R. J. (1996) "Deterministic sliding block methods for estimating seismic displacements of earth structures." *Soil Dyn. and Earthq. Engrg.*, 15, 255-268.

Franklin, A. G., and Chang, F. K. (1977). "Earthquake resistance of earth and rockfill dams." *Misc. Paper S-71-17*, U.S. Army Waterway Experiment Station, Vicksburg, Miss.

Hynes-Griffin, M.E., and Franklin, A.G. (1984). "Rationalizing the seismic coefficient method." *Misc. Paper GL-84-13*, U.S. Army Waterway Experiment Station, Vicksburg, Miss.

Jibson, R.W. (1994). "Predicting earthquake-induced landslide displacements using Newmark's sliding block analysis." *Trans. Res. Rec.* 1411, 9-17.

Jibson, R.W., Harp, E.L., Michael, J.A. (1998). "A method for producing digital probabilistic seismic landslide hazard maps: an example from the Los Angeles California area." *USGS Open-File Rep. 98-113*.

Jibson, R.W., Harp, E.L., Michael, J.A. (2000). "A method for producing digital probabilistic seismic landslide hazard maps." *Engrg Geol*., 58(3-4), 271–289.

Newmark, N. M. (1965). "Effects of earthquakes on dams and embankments." *Geotechnique,* 15(2), 139-160.

Makdisi, F. I., and Seed, H. B. (1978). "Simplified procedure for estimating dam and embankment earthquake-induced deformations." *J. Geotech. Eng.,* 104(7), 1427-1434.

Richards, R. & Elms, D. G. (1979). "Seismic behavior of gravity retaining walls." *J. Geotech. Engng Div., ASCE,* 105(GT4), 449-464.

Sarma, S.K. (1975). "Seismic stability of earth dams and embankments." *Geotechnique,* 25(4), 743-761.

Whitman, R.V. & Liao, S. "Seismic design of gravity retaining walls." *Proc. of the 8th World Conf.on Earthq. Engrg.*, San Francisco, 3, 533-540.

Whitman, R.V. & Liao, S. (1985). "Seismic design of retaining walls." *Misc. Paper GL-85-1*, U.S. Army Waterway Experiment Station, Vicksburg, Miss.

Yegian, M. K., Marciano, E. A., and Ghahraman, V. G. (1991). "Earthquake-induced permanent deformations: probabilistic approach." *J. Geotech. Eng.,* 117(1), 35-50.


### Analytical rigid-block methods


Newmark, N. M. (1965). "Effects of earthquakes on dams and embankments." *Geotechnique,* 15(2), 139-160.

GeoSyntec. (1996). *User's manual for YSLIP–PM*, Huntington Beach, Calif.

**Deterministic decoupled methods**

Bray, J. D., Rathje, E. M., Augello, A. J., and Merry, S. M. (1998). "Simplified seismic design procedure for lined solid-waste landfills." *Geosynthet. Int..,* 5(1-2), 203–235.

Bray, J.D., and Rathje, E.M., (1998). "Earthquake-induced displacements of solid-waste fills." *J. Geotech. and Geoenvir. Engrg*., 124(3), 242-253.

Hynes-Griffin, M.E., and Franklin, A.G. (1984). "Rationalizing the seismic coefficient method." *Misc. Paper GL-84-13*, U.S. Army Waterway Experiment Station, Vicksburg, Miss.

Makdisi, F. I., and Seed, H. B. (1978). "Simplified procedure for estimating dam and embankment earthquake-induced deformations." *J. Geotech. Eng.,* 104(7), 1427-1434.

**Analytical decoupled methods**

Chopra, A.K. (1967). "Earthquake response of earth dams." *J. Soil Mech. and Found. Div.* 90(SM2): 65-81.

GeoSyntec. (1996). *User's manual for YSLIP–PM*, Huntington Beach, Calif.

Itasca Consulting Group. (2005). *FLAC – Fast Lagrangian Analysis of Continua, Version 5 User's Manual*. Minneapolis, Minn.

Makdisi, F. I., and Seed, H. B. (1978). "Simplified procedure for estimating dam and embankment earthquake-induced deformations." *J. Geotech. Eng.,* 104(7), 1427-1434.

Seed, H.B. and Martin, G.R. (1966). "The seismic coefficient in earth dam design." *J. Soil Mech. and Found. Div.*, ASCE, 92(SM3), 25-58.

**Fully-coupled methods**

Itasca Consulting Group. (2005). *FLAC – Fast Lagrangian Analysis of Continua, Version 5 User's Manual*. Minneapolis, Minn.